

# Al<sup>3+</sup> Impacting on Eu<sup>3+</sup> - Host Energy Transfer and Calculation of Eu<sup>3+</sup> <sup>5</sup>D<sub>0</sub> Quantum Efficiency

Fabin, Cao <sup>a,\*</sup>

Anhui Provincial Key Laboratory for Metallurgical Engineering & Resources Recycling, Anhui University of Technology

Anhui University of Technology, AHUT  
Maanshan, Anhui, 243002, PR China

email: fbcao@ahut.edu.cn, yjsun7410@aliyun.com

Luhong Wei

Anhui Provincial Key Laboratory for Metallurgical Engineering & Resources Recycling, Anhui University of Technology

Anhui University of Technology, AHUT  
Maanshan, Anhui, 243002, PR China

email: 541354376@qq.com

**Abstract**—With 2 mol% Al<sup>3+</sup> ions and 8 mol% Eu<sup>3+</sup> ions co-doping, nano-size [K<sub>0.8</sub>Y<sub>0.63</sub>Eu<sub>0.37</sub>Al<sub>0.02</sub>][Mo<sub>0.2</sub>W<sub>0.8</sub>O<sub>4</sub>] phosphor was synthesized by the sol-gel method. Through XRD, DTA-TG, SEM and photoluminescent analysis, its morphology, crystal structure and luminescent property were discussed and it is found that one type of excellent phosphor can be obtained, and its luminescent efficiency and particles sizes can be improved to some extent by adjusting suitable technological conditions. According to the photoluminescent characteristics of the phosphor, its emission mechanism was mentioned. The partial J-O parameters and quantum efficiency of Eu<sup>3+</sup> <sup>5</sup>D<sub>0</sub> energy level were calculated under 395 nm excitation. The phosphor can combine with 390–410 nm InGaN chip in order to get different simple color light and white light. Under 20 mA forward-bias current, bright red light is observed by naked eyes so the phosphor will have excellent application outline from the LED illumination and display in the further.

**Keywords**—co-doping; energy transfer; J-O parameters; quantum efficiency; red LED

## I. INTRODUCTION

To date, many efforts have been devoted to develop high-efficient red phosphors [1-3]. In particular, Eu<sup>3+</sup> ions doped molybdates and tungstates in near-UV-based LEDs application have attracted many interests because of their remarkable red-luminescence properties, such as Eu<sub>2</sub>WO<sub>6</sub>, NaEu(MoO<sub>4</sub>)<sub>2</sub> [2], (Ca, Sr)(Mo, W)O<sub>4</sub>, and K<sub>5</sub>Eu(MoO<sub>4</sub>)<sub>4</sub>, which are very favorable to not suffer from high photon flux and luminescence quenching in application. However, there are still big challenge for their luminescent efficiency [4].

To solve those problems, (Li/Na, Y, Eu)(Mo, W)O<sub>4</sub>, (Na, Gd, Eu)(Mo, W)O<sub>4</sub>, (Ca, Sr, Eu<sup>3+</sup>)MoO<sub>4</sub> and (Ca, Sr, Eu<sup>3+</sup>, Sm/Gd/Y/La)(Mo, W)O<sub>4</sub> were prepared and charge compensation impact on the its luminescent intensity was investigated in our previous research work [5-8]. It is found that their luminescent efficiency can be improved to some degree. In this paper, [K<sub>0.8</sub>Y<sub>0.63</sub>Eu<sup>3+</sup>Al<sub>0.02</sub>][Mo<sub>0.2</sub>W<sub>0.8</sub>O<sub>4</sub>] was prepared by co-precipitation method and it is found that Al<sup>3+</sup>-Eu<sup>3+</sup> energy transfer existing in

the host can improve its emission ability and its quantum efficiency and partial J-O parameters were calculated in detail.

## II. EXPERIMENTAL METHODS

Eu<sup>3+</sup>-Al<sup>3+</sup> co-doped [K<sub>0.8</sub>Y<sub>0.63</sub>Eu<sub>0.37</sub>Al<sub>0.02</sub>][Mo<sub>0.2</sub>W<sub>0.8</sub>O<sub>4</sub>](KYEAMW) (total amount, 0.005 mol) was prepared by co-precipitation. A mixture of stoichiometric KNO<sub>3</sub>(AR), Y(NO<sub>3</sub>)<sub>3</sub>(AR), Eu(NO<sub>3</sub>)<sub>3</sub>(99.99%purity, 8 mol%), and Al(NO<sub>3</sub>)<sub>3</sub> (AR, 2mol%) was dissolved in 30 ml distilled water. Ammonium molybdate ((NH<sub>4</sub>)<sub>6</sub>Mo<sub>7</sub>O<sub>24</sub>·4H<sub>2</sub>O, AR) and ammonium tungstate ((NH<sub>4</sub>)<sub>10</sub>H<sub>2</sub>(W<sub>2</sub>O<sub>7</sub>)<sub>6</sub>, AR) were dissolved in 50 ml distilled water and the PH of solution was adjusted to 1.2-1.4 with diluted HNO<sub>3</sub>. The Eu<sup>3+</sup>-Al<sup>3+</sup> solution was slowly poured into W-Mo solution dropwise to form a clear and homogeneous solution. The solution was neutralized with precipitation agents (NH<sub>4</sub>)<sub>2</sub>CO<sub>3</sub> and deposit the precursor at 78. The precursor was washed in distilled water several times and put into the drying cabinet for drying at 90 °C for 2 hours. Finally, the dried and ground it into power, namely KYEAMW. All reagents were bought from Sinopharm Chemical Reagent Co.,Ltd.

The structure of KYEAMW was recorded by X-ray powder diffraction(XRD) employing CuK<sub>α</sub> radiation at 40kv and 250mA. A step size of 0.02 degree (2theta) was used with a scan speed of 4 degrees/min. Thermo-gravimetric analysis (TG) and differential thermal analysis (DTA) were carried out simultaneously using a TG-DTA92 instrument (SETARAM, France). About 5 mg the precursor of KYEAMW were weighed in alumina crucible and first isothermally heated to 30°C for 2 min, and subsequently heated from 30 to 1050°C in a dynamic air atmosphere (air flow 5 L/h). The heating rate was 15°C / min. The furnace was calibrated using transition temperature of indium and aluminum. Calcined caolinities were used as reference materials. Excitation and emission spectra were measured by using a Hitachi F-4600 spectrometer equipped with a 150 W-xenon lamp under a working voltage of 500 V. The excitation and

emission slits were set at 2.5 nm and scanning speed was 1200nm/min. All the measurements were performed at room temperature.

### III. RESULTS AND DISCUSSION

Fig .1(a) indicates the XRD pattern of KYEAMW, of which the crystal structure is consistent with JCPDS card No. 29-0351, corresponding to the intrinsic diffraction patterns of  $\text{CaMoO}_4$ , a tetragonal crystal structure with space group of  $I4_1/a(88)$ . Fig .1(b) depicts the TG-DTA curves of the precursor of KYEAMW. The first weight loss stage is from room temperature to 700°C or so, corresponding to the endothermic peak at about 415 °C, which is associated with water loss and gel decomposed into oxides with network structure. The second weight loss stage is no weight loss from 700 to 1050 °C, corresponding to the endothermic peak at 820 °C or so, which is attributed to the crystallization and crystal particles growth of KYEAMW.

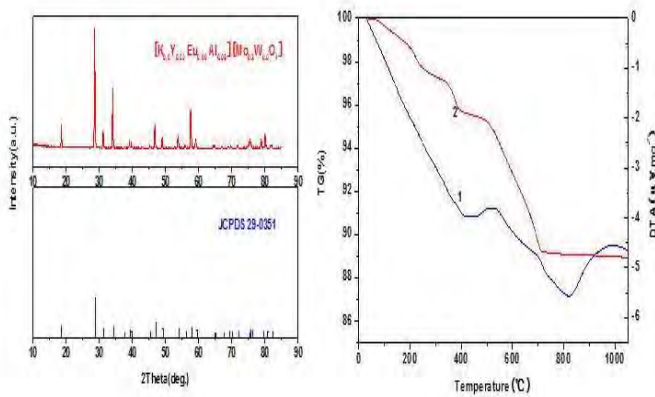


Figure 1. XRD pattern of KYEAMW(a) and DTA curve(1) and TG curve(2) of the precursor of KYEAMW(b)

Fig .2(a) presents excitation spectrum of KYEAMW under 614 nm monitoring and its emission spectrum under 395nm excitation. In the left excitation spectrum, there are one broad band from 200 nm to 450 nm(303.4 nm from  $\text{O}^{2-} \rightarrow \text{Mo}^{6+}/\text{W}^{6+}/\text{Eu}^{3+}$  transition, 362.4 nm from  ${}^7\text{F}_0 \rightarrow {}^5\text{D}_4$  transition, 376.2 nm from  ${}^7\text{F}_0 \rightarrow {}^5\text{L}_7$  transition, 394.6 nm from  ${}^7\text{F}_0 \rightarrow {}^5\text{L}_6$  transition, and 415.4 nm from  ${}^7\text{F}_0 \rightarrow {}^5\text{D}_3$  transition) and two sharp peaks, respectively, corresponding to  ${}^7\text{F}_0 \rightarrow {}^5\text{D}_2$ (splitting, 450, 465.4 , 472.8 , and 487.8 nm) transition and  ${}^7\text{F}_0 \rightarrow {}^5\text{D}_1$ (splitting, 526.8 and 534.6 nm) transition.  $\text{O}^{2-} \rightarrow \text{Mo}^{6+}/\text{W}^{6+}/\text{Eu}^{3+}$  transition originates from the charge transfer( abbreviation, CT) transitions of  $\text{MoO}_6$ ,  $\text{WO}_6$  and  $\text{EuO}_6$ [9]. According to ref[10], it is determined for the  $\text{MoO}_6$  groups CT band covering 225-375 nm and the  $\text{WO}_6$  groups locating around 250-330 nm. Referring to the data reported in other  $\text{Eu}^{3+}$  doped phosphors[11], the CT band of  $\text{EuO}_6$  should be located around 250-320 nm. In the right emission spectrum of KYEAMW under 395 nm excitation, there are seven peaks attributed to  ${}^5\text{D}_0 \rightarrow {}^7\text{F}_0$  (581 nm/193 a.u.),  ${}^5\text{D}_0 \rightarrow {}^7\text{F}_1$  (590.2 nm/874 a.u. and 595.8 nm/1119 a.u.),  ${}^5\text{D}_0 \rightarrow {}^7\text{F}_2$ (613.6 nm/5316 a.u. and 631.2 nm/411 a.u.),  ${}^5\text{D}_0 \rightarrow {}^7\text{F}_3$ (657.6nm/176 a.u.), and  ${}^5\text{D}_0 \rightarrow {}^7\text{F}_4$ (680 nm/34 a.u., 693.2 nm/107 a.u. and 708.4 nm/439 a.u.) in TABLE I.  ${}^5\text{D}_0 \rightarrow {}^7\text{F}_{2,4,6}$  transitions are electric dipole transitions and  ${}^5\text{D}_0 \rightarrow {}^7\text{F}_1$  transition is

magnetic dipole transitions.  ${}^5\text{D}_0 \rightarrow {}^7\text{F}_{3,5}$  are both magnetic dipole (MD) transitions and electric dipole (ED) transitions. In theory, ED transitions are generally forbidden since the parity does not allow the transition because 5d and 4f have opposite parities. But in the experiments, the forbidden is partly relieved because  $\text{Eu}^{3+}$  occupies a non-central-symmetric site when  $\text{Eu}^{3+}$  was doped in the host so narrow emission peaks are presented, corresponding to  ${}^5\text{D}_0 \rightarrow {}^7\text{F}_{2,4}$  transitions.

TABLE I. The average energies (cm-1) and emission peaks situation/area of  $\text{Eu}^{3+} 5\text{D}_0 \rightarrow 7\text{F}_J(J=0-4)$  of KYEAMW/KYEMW

transitions	Energy ( $\nu_{0-i}$ , cm <sup>-1</sup> )	EM area( $S_{0-i}$ )	EM situation( $\lambda_i$ , nm)
${}^5\text{D}_0 \rightarrow {}^7\text{F}_0$	17212/17212	871/858	581/581
${}^5\text{D}_0 \rightarrow {}^7\text{F}_1$	16943, 16784/	10909/	590.2, 595.8/
	16949, 16784	9982	590, 595.8
${}^5\text{D}_0 \rightarrow {}^7\text{F}_2$	16297, 15843/	46874/42539	613.6, 631.2/613.6, 631.3
	16297, 15840		
${}^5\text{D}_0 \rightarrow {}^7\text{F}_3$	15207/15207	2463/2057	657.6/576.6
${}^5\text{D}_0 \rightarrow {}^7\text{F}_4$	14706, 14426, 14116	5535/5033	680, 693.2, 708.4/680,
	/14706, 14430, 14114		693, 708.5

Fig .2(b) shows emission spectra of KYEAMW and KYEMW under 395nm excitation. With  $\text{Al}^{3+}$  ions doped or not in the host, the luminescent intensity increases 112.4 %. But no emission peaks of  $\text{Al}^{3+}$  ions exist in the emission spectra. So it is sure that  $\text{Al}^{3+}$  ions play an important role in the procedure of energy transfer between the host and  $\text{Eu}^{3+}$  ions. Fig .2(C) depicts the energy transfer path diagram of the host  $\rightarrow \text{Eu}^{3+}$  in 2 mol%  $\text{Al}^{3+}$  ions and 8 mol%  $\text{Eu}^{3+}$  co-doped YKEAMW. For the CT excitation of YKEAMW phosphor, the optical centers are composed of central  $\text{Eu}^{3+}$  ions binding with their ligands  $-\text{O}^{2-}$  ions and the host is composed of central  $\text{Mo}^{6+}/\text{W}^{6+}$  ions binding with  $\text{O}^{2-}$  ions. In the breathing model of the optical center, the ligand pulsates, away from the central ion, and a harmonic oscillator mode can describe the pulsations. The energy of the optical center, including the vibrational energy of the ligand, is depicted by lines in the configurational coordinate diagram (CCD).

There are series of parallel lines labeled  ${}^7\text{F}_0, {}^7\text{F}_1, \dots; {}^5\text{D}_0, {}^5\text{D}_1, {}^5\text{D}_2, {}^5\text{D}_3, \dots$  in Fig .2(c), denoting the energy states of the optical center when the central  $\text{Eu}^{3+}$  ion is in its different  $4f^6$  levels. The spectrum contains sharp lines at 613.6 and 595.8 nm derived from ED and MD transitions of  $\text{Eu}^{3+}$  ion, respectively. However, no emission corresponding to tungstate or molybdate is observed. Red emission due to  $\text{Eu}^{3+}$  is observed under CT excitation, which clearly indicates the energy transfer from tungstate or molybdate group to  $\text{Eu}^{3+}$  levels. However, the relative PL intensity of  $\text{Eu}^{3+}$  is more with CT band excitation when compared with that due to  $\text{Eu}^{3+}$  excitation.[12] This reveals that the energy from host lattice to  $\text{Eu}^{3+}$  is competent. Generally the  $\text{Eu}^{3+}$  emission lines are hypersensitive, that is, they are highly sensitive to the crystal chemical environment.[13] ED transition is dominant when  $\text{Eu}^{3+}$  occupies non-centrosymmetric site in the lattice.[14] In the present study, the relative intensity of ED transition is found to be high. It clearly

indicates that the  $\text{Eu}^{3+}$  ion occupies non-centrosymmetric site in KYEAMW.

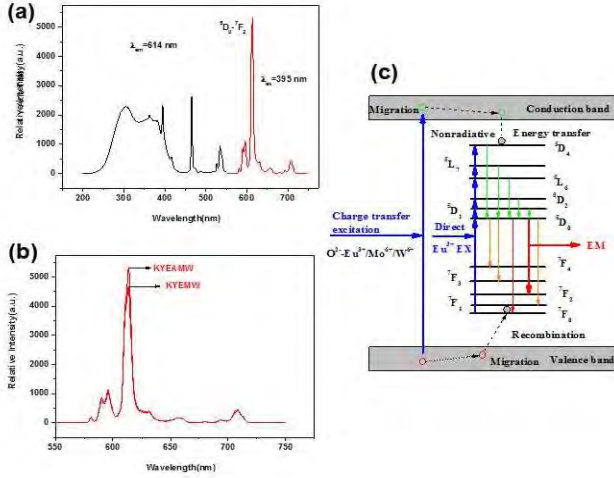


Figure 2. Excitation spectrum of KYEAMW under 614 nm monitoring and its emission spectrum under 395 nm excitation(a); and Emission spectra of KYEAMW and KYEMW under 395 nm excitation(b); and Energy transfer path diagram of the host  $\rightarrow \text{Eu}^{3+}$  in KYEAMW(c).

As far as the  $\text{Eu}^{3+} {}^5\text{D}_0 \rightarrow {}^7\text{F}_J$  ( $J = 0 - 6$ ) transition is concerned,  ${}^5\text{D}_0 \rightarrow {}^7\text{F}_1$  magnetic dipole transition,  ${}^5\text{D}_0 \rightarrow {}^7\text{F}_{2,4,6}$  electric dipole transitions,  ${}^5\text{D}_0 \rightarrow {}^7\text{F}_{3,5}$  contain both electric dipole and magnetic dipole transition components.  ${}^5\text{D}_0 \rightarrow {}^7\text{F}_{5,6}$  transitions are forbidden for both electric dipole and magnetic dipole transitions and farther in the infrared region. So the emission of  ${}^5\text{D}_0 \rightarrow {}^7\text{F}_{5,6}$  transitions cannot be observed in the experiments.

In order to characterize transition rate between different energy levels of  $\text{Eu}^{3+}$  ions, two transition intensity parameters  $\Omega_\lambda$  ( $\lambda = 2, 4$ ), called J-O parameters, are introduced into Judd-Ofelt theory.  $\Omega_\lambda$  can be influenced by environment around  $\text{Eu}^{3+}$  ions. Especially,  $\Omega_2$  has a close relationship to the environment around  $\text{Eu}^{3+}$  ions. For K-Y-Mo-W host,  $\Omega_2$  reflects structure symmetry, order property and covalent character of K-Y-Mo-W interaction. In a word, the host system which has larger  $\Omega_2$  is in a more polarizable chemical environment and has stronger covalent character of K-Y-Mo-W interaction. Thus, transition intensity parameters can help us to know the lattice-sites occupied by  $\text{Eu}^{3+}$  ions in K-Y-Mo-W host and the micro-environment around  $\text{Eu}^{3+}$  ions.

Quantum efficiency of  $\text{Eu}^{3+} {}^5\text{D}_0$  energy level can also be calculated by experimental data. The fluorescence lifetime  $\tau$  of  ${}^5\text{D}_0$ , radiative transition rate  $A_R$  and non-radiative transition rate  $A_N$  can be expressed as follows.

$$\frac{1}{\tau} = A_R + A_N \quad (1)$$

where  $A_R$  is the sum of each  ${}^5\text{D}_0 \rightarrow {}^7\text{F}_J$  ( $J = 1, 2, 4$ ) transition rate, viz.  $\sum_{J=1,2,4} A_{0-J} = A_{0-1} + A_{0-2} + A_{0-4} = A_R$ .

The  $A_{0-J}$  values are obtained by using the relation:  $A_{0-J} = A_{0-1} (S_{0-J} / S_{0-1}) (\nu_{0-J} / \nu_{0-1})$ , where  $S_{0-J}$  is the area under the curve related to the  ${}^5\text{D}_0 \rightarrow {}^7\text{F}_J$  transition obtained from the spectral data,  $\nu_{0-J}$  is the

energy barycenter of the 0-J transition. Here  $A_{0-J}$  is the experimental coefficients of spontaneous emissions,  $A_{0-1}$  is the Einstein's coefficient of spontaneous emission between the  ${}^5\text{D}_0$  and  ${}^7\text{F}_1$  energy levels, which can be determined as approximately  $50 \text{ s}^{-1}$  and as a reference to calculate the value of other  $A_{0-J}$  [16-17]. So the quantum efficiency of  $\text{Eu}^{3+} {}^5\text{D}_0$  energy level can be expressed by

$$\eta = \frac{A_R}{A_R + A_{NR}} = \tau \sum_{J=1,2,3,4} A_{0-J} \quad (2)$$

Fluorescence decay curves (measuring luminescence of  ${}^5\text{D}_0 \rightarrow {}^7\text{F}_2$ ) of  ${}^5\text{D}_0$  energy level are measured under 395 nm excitation. The fluorescence decay curves are fitted by exponential decay to obtain the values of  $\tau$ . Then the value of  $\eta$  would be obtained by Eq. (2). TABLE II depicts the average energies ( $\text{cm}^{-1}$ ) and emission peaks situation/area of  $\text{Eu}^{3+} {}^5\text{D}_0 \rightarrow {}^7\text{F}_J$  ( $J=0-4$ ) of KYEAMW and TABLE II shows the values of  $\tau$ ,  $A_R$ ,  $A_R + A_N$ ,  $\eta$  and so on of KYEAMW. According to Judd-Ofelt theory,  ${}^5\text{D}_0 \rightarrow {}^7\text{F}_1$  magnetic dipole transition rates can be represented by  $A_{0-1}$  is the Einstein's coefficient of spontaneous emission from  ${}^5\text{D}_0 \rightarrow {}^7\text{F}_1$ , which can be determined as approximately  $50 \text{ s}^{-1}$  and as a reference to calculate the value of other  $A_{0-J}$  [15-16].

$$\begin{aligned} A_{0-1} &= 50 \text{ s}^{-1}, \\ A_{0-0} &= A_{0-1} (S_{0-0} / S_{0-1}) (\nu_{0-0} / \nu_{0-1}) = 4.1 \text{ s}^{-1}, \\ A_{0-2} &= A_{0-1} (S_{0-2} / S_{0-1}) (\nu_{0-2} / \nu_{0-1}) = 204.7 \text{ s}^{-1}, \\ A_{0-4} &= A_{0-1} (S_{0-4} / S_{0-1}) (\nu_{0-4} / \nu_{0-1}) = 21.7 \text{ s}^{-1}, \\ A_R &= A_{0-0} + A_{0-1} + A_{0-2} + A_{0-4} = 280.5 \text{ s}^{-1} \\ A_R + A_N &= 1/\tau = 1000/0.558 = 1792.1 \text{ s}^{-1} \\ \eta &= A_R / (A_R + A_N) * 100\% = 15.7\% \end{aligned}$$

TABLE II. Partial J-O parameters, fluorescence lifetime, transition rates and quantum efficiency of KYEAMW and KYEMW under 395 nm excitation

PL	KYEMW	KYEAMW
$\Omega_2 (10^{-20} \text{ cm}^2)$	5.40	5.46
$\Omega_4 (10^{-20} \text{ cm}^2)$	1.40	1.45
$A_{0-J}$	4.39, 50, 203.0, 21.55	4.1, 50, 204.7, 21.7
$\tau$ (ms)	0.499	0.558
$A_R$ ( $\text{s}^{-1}$ )	278.94	280.5
$A_N$ ( $\text{s}^{-1}$ )	1725.06	1511.6
$A_R + A_N$ ( $\text{s}^{-1}$ )	2004	1792.1
$\eta\%$	13.92	15.7

The  ${}^5\text{D}_0 \rightarrow {}^7\text{F}_J$  ( $J = 2, 4$ ) is electric dipole transition, so the radiative transition rate (total electric dipole transition) can be expressed as follows.

$$A_{0-J} = \frac{64\pi^4 e^2 k_J^3 n(n^2 + 2)^2}{3h(2J' + 1) 9} \Omega_J \langle \psi' J' \| U^\lambda \| \psi J \rangle^2 \quad (3)$$

where  $e$  is elementary charge,  $k_J$  wavenumber of electric dipole transition luminescence,  $J'$  equaling zero for the  ${}^5\text{D}_0 \rightarrow {}^7\text{F}_J$ ,  $\Omega_\lambda$  transition intensity parameter, and

$\langle \psi J \| U^\lambda \| \psi' J' \rangle^2$  is squared reduced matrix element of transition from  $|\psi' J'\rangle$  to  $|\psi J\rangle$ .

Thus the ratio between electric dipole transition rate and magnetic dipole transition rate can be expressed as follows.

$$\frac{A_{0-J}}{A_{md}} = \frac{e^2 k_J^3}{S_{md} k_{md}^3} \frac{(n^2 + 2)^2}{9n^2} \Omega_J \langle \psi J \| U^\lambda \| \psi' J' \rangle^2 \quad (4)$$

Transition rate of each energy level is in direct proportion to integral intensity of emission spectrum in Table I. where  $k_{md}$  is wavenumber of  ${}^5D_0 \rightarrow {}^7F_1$  luminescence and  $k_J$  is wavenumber of  ${}^5D_0 \rightarrow {}^7F_J$ ,  $n$  refractive index of host 1.6 [17],  $h$  Planck constant,  $J'$  equaling zero for the  ${}^5D_0 \rightarrow {}^7F_1$ , and  $S_{md}$  is line strength of  ${}^5D_0 \rightarrow {}^7F_1$  transition. Because linear strength of magnetic dipole transition nearly can't be influenced by outer environment, the value of  $S_{md}$  for a certain transition has no relation with the hosts and it is a constant.  $S_{md}$  is calculated to be  $7.83 \times 10^{-42}$  esu(c)  $\text{cm}^2$  through the data in literature [18].  $\langle \psi J \| U^\lambda \| \psi' J' \rangle^2$  values are the square reduced matrix elements whose values are 0.0032 and 0.0023 for  $J=2$  and  $4$  [16]. All parameters in this section used Gauss system of units. Then, according to Eq. (4),  $\Omega_J$  can be calculated by utilizing emission spectrum. Table 3 shows the values of  $\Omega_2$  and  $\Omega_4$  ( $\Omega_2=5.46 \times 10^{-20}(\text{cm}^2)$  and  $\Omega_4=1.45 \times 10^{-20}(\text{cm}^2)$ ). Moreover, the higher emission quantum efficiency is obtained from the KYEAMW phosphors ( $\eta=15.7\%$ ) than in KYEMW phosphors ( $\eta = 13.92\%$ ), which is due to appreciably decrease in non-radiative decay rates from the  ${}^5D_0$  level.

#### IV. CONCLUSIONS

With 2 mol %  $\text{Al}^{3+}$  ions and 8 mol%  $\text{Eu}^{3+}$  ions co-doping  $[\text{K}_{0.8}\text{Y}_{0.63}\text{Eu}^{3+}_{0.08}\text{Al}_{0.02}][\text{Mo}_{0.2}\text{W}_{0.8}\text{O}_4]$  nano-powder with good luminescent properties can be synthesized by co-precipitation method and its possible energy transfer mechanism are mentioned. According to the characteristics of reduced matrix for  ${}^5D_0 \rightarrow {}^7F_{2,4}$

transitions, J-O transition parameters  $\Omega_2$  and  $\Omega_4$  can be calculated,  $\Omega_2=5.46 \times 10^{-20}(\text{cm}^2)$  and  $\Omega_4=1.45 \times 10^{-20}(\text{cm}^2)$ , and energy transfer efficiency between  $\text{Eu}^{3+}$  ions and  $\text{WO}_4/\text{MoO}_4$  groups is improved,  $\eta = 15.7\%$  (compared to  $[\text{K}_{0.8}\text{Y}_{0.65}\text{Eu}^{3+}_{0.08}][\text{Mo}_{0.2}\text{W}_{0.8}\text{O}_4]$ ,  $\eta = 13.92\%$ ).

#### ACKNOWLEDGMENT

The authors are grateful for the Natural Science Foundation of Anhui Provincial Science and Technology Agency (No. 1408085ME78) of PR China.

#### REFERENCES

- [1] Haque M., Kim D.K. Mater. Lett. 2009; 63(9-10): 793.
- [2] Wang Z., Liang H., Gong M., Su Q. Mater. Lett. 2008; 62(4-5):619.
- [3] Zhang X., Chen H., Kim J. J. Rare Earth, 27 , 50 ( 2009).
- [4] Hajime Y., Hidetsugu M. Proc. SPIE, 1995; 2362(2): 612.
- [5] Cao F.B., Tian Y.W., Chen Y.J., Xiao L.J., Wu Q. J. Lumin. 2009; 129(6): 585.
- [6] Cao F.B., Tian Y.W., Chen Y.J., Xiao L.J., Wu Q. J. Alloys Compd. 2009; 475(1-2):387.
- [7] Cao F.B., Chen Y.J., Tian Y.W., Xiao L.J., Li L.K. J. Nanosci. Nanotechnol. 2010; 10(3): 2060.
- [8] Cao F.B., Li L.X., Tian Y.W., Wu X.R., Chen Y.J., Xiao L.J. Appl. Spectrosc. 2010; 64(11):1298.
- [9] Sheu J. K., Chang S. J., Kuo C. H., Su Y. K., Wu L. W., Lai Y. C., et al. IEEE Photonics Technol. Lett. 2003; 15(1):18.
- [10] Huh Y., Shim J., Kim Y., Rag Do Y. J. Electrochem. Soc. 2003; 150(2):H57.
- [11] Wang Z., Liang, H., Gong M., Su Q. Electrochem. Solid Stat. 2005; 8(4): H33.
- [12] Sivakumar V., Varadaraju U. V. J. Electrochem. Soc. 2005; 152(10): H168.
- [13] Katzin L. I. Inorg. Chem. 1969; 8(8):1649.
- [14] Blasse G., Grabmaier B. C. Luminescent Materials, Springer-Verlag, Berlin, 1994.
- [15] Lin Y.H., Tang Z.L., Zhang Z.T. J. Alloys Compd. 2003; 348(1-2):76.
- [16] Lei F., Yan B. J. Solid State Chem. 2008; 181(4):855.
- [17] Teotonio E.E.S., Espinola J.G.P., Brito H.F., Malta O.L., Oliveria S.F., de Faria D.L.A., Izumi C.M.S. Polyhedron 2002; 21(18):1837.
- [18] Boyer J.C., Vetrone F., Capobianco J.A., Speghini A., Bettinelli M. J. Phys. Chem. B. 2004; 108(52): 20137.